Poly(vinylidene fluoride-*co*-hexafluoropropylene) (PVDF-*co*-HFP) Hollow Fiber Membranes Prepared from PVDF-*co*-HFP/PEG-600Mw/DMAC Solution for Membrane Distillation

Qusay F. Alsalhy,[1] Khalid T. Rashid,[1] Salah S. Ibrahim,[1] Abdulsattar H. Ghanim,[1] Bart Van der Bruggen,[2] Patricia Luis,[2] Mumtaz Zablouk[1]

[1]Chemical Engineering Department, University of Technology, Baghdad, Iraq
[2]Department of Chemical Engineering, K.U. Leuven, Leuven, Belgium
Correspondence to: Q. F. Alsalhy (E-mail: qusay_alsalhy@yahoo.com) or (E-mail: qusayalsalhy@uotechnology.edu.iq)

ABSTRACT: Poly(vinylidene fluoride-*co*-hexafluoropropylene) (PVDF-*co*-HFP) hollow fiber membranes were prepared by using the phase inversion method. The effect of polyethylene glycol (PEG-600Mw) with different concentrations (i.e., 0, 5, 7, 10, 12, 15, 18, and 20 wt %) as a pore former on the preparation and characterization of PVDF-*co*-HFP hollow fibers was investigated. The hollow fiber membranes were characterized using scanning electron microscopy, atomic force microscopy, and porosity measurement. It was found that there is no significant effect of the PEG concentration on the dimensions of the hollow fibers, whereas the porosity of the hollow fibers increases with increase of PEG concentration. The cross-sectional structure changed from a sponge-like structure of the hollow fiber prepared from pure PVDF-*co*-HFP to a finger-like structure with small sponge-like layer in the middle of the cross section with increase of PEG concentration. A remarkable undescribed shape of the nodules with different sizes in the outer surfaces, which are denoted as "twisted rope nodules," was observed. The mean surface roughness of the hollow fiber membranes decreased with an increase of PEG concentration in the polymer solution. The mean pore size of the hollow fibers gradually increased from 99.12 to 368.91 nm with increase of PEG concentration in polymer solution. © 2013 Wiley Periodicals, Inc. J. Appl. Polym. Sci. 129: 3304–3313, 2013

INTRODUCTION

During the last decade, poly(vinylidene fluoride-*co*-hexafluoro-propylene) (PVDF-*co*-HFP) has been recognized as an excellent material for preparation of membrane distillation (MD) membranes: it has an excellent thermal stability and chemical and abrasion resistance, and it is self-extinguishing and retains properties on aging.[1–6] The most important characteristics of membranes desired for MD are pore size, pore size distribution, porosity, and membrane thickness. The permeation flux increases with increasing membrane pore size and porosity and decrease of the membrane thickness. Moreover, a narrow pore size distribution of the membrane avoids wetting of the large pore sizes, which leads to a decrease of the retention.[7] Therefore, several researchers focused their work on improving the membrane specifications in order to enhance the MD performance by drastically altering the membrane morphology. For example, Feng et al.,[1,2] studied the effects of LiCl and LiClO₄·3H₂O/tri-methyl phosphate as a pore-forming additive on the permeabil-ity of PVDF-*co*-HFP membranes. They found that the additives increased the average pore size and porosity of the membrane, and thus, a higher permeate flux is attained. PVDF-*co*-HFP porous membranes were prepared from polyethylene glycol (PEG) serial additives by Feng et al.[3] PVDF-*co*-HFP membranes exhibited high water permeability, but the dry membrane shows a low rejection in direct contact membrane distillation (DCMD) due to the existence of residual additives in the membrane ma-trix. Khayet et al.[6] prepared PVDF-*co*-HFP membranes using dif-ferent polymer concentrations, PEG-10kDa as additives, a range of coagulation temperatures, and solvent evaporation times for application in DCMD. They found that the fluxes increased with increase of the PEG concentration and decrease of the PVDF-*co*-HFP concentration, the coagulation temperature, and the sol-vent evaporation time. This result is attributed to large pore size, high porosity, low thickness, and high mean roughness.

Most researchers cited above have used different additives for the preparation of PVDF-*co*-HFP membranes such as poly(vinyl

pyrrolidone) (PVP), PEG, LiCl, glycerol, and water in order to induce copolymer precipitation during the passage of nascent fiber through the external coagulation bath. According to the literature, there is no report on the preparation of PVDF-*co*-HFP hollow fiber membranes without additives. In this study, the preparation of PVDF-*co*-HFP hollow fiber membranes with and without additives is described. The effect of the PEG-600Mw concentration as a pore-forming additive on the desired characteristics of the PVDF-*co*-HFP hollow fiber membrane prepared for MD application by phase inversion was investigated. The choice of the additive concentrations was as broad as possible, to maximize the understanding of the effect of the pore former. PEG as a pore former was used in different concentrations as additive: 0, 5, 7, 10, 12, 15, 18, and 20 wt %. In the literature, values for pore former addition are typically in a similar although more narrow range. For example, Wongchitphimon et al.[8] used concentrations of a pore former (PEG in that case) of 3%, 5%, and 10%. We were mainly interested in the high end of this range, but with a broad distribution. Morphological studies of the PVDF-*co*-HFP hollow fibers were conducted by scanning electron microscopy (SEM) and atomic force microscopy (AFM).

EXPERIMENTAL WORK

Materials
PVDF-*co*-HFP (number-average molecular weight, 120,000) was purchased from Sigma–Aldrich Chemical Company (Germany). *N,N*-Dimethyl acetamide (DMAC) and PEG (Mw =600 Da) were used as a solvent and additive, respectively. All chemicals were purchased from Sigma–Aldrich Chemical Company.

Preparation of Hollow Fiber Membrane
PEG with different concentrations as additive (0, 5, 7, 10, 12, 15, 18, and 20 wt %) was first dissolved in solvent DMAC. Then, PVDF-*co*-HFP was added to the mixture at 40°C. The polymer solution was kept under constant stirring at 40°C until the mixture was homogeneous. The homogeneous PVDF-*co*-HFP solution was kept in a vertical column pressurized by pure nitrogen and degassed for about 24 h at 35°C. The nitrogen pressure on the PVDF-*co*-HFP solution column was adjusted to 2 bars. The spinneret used has 500 μm inner diameter and 900 μm outer diameter. The PVDF-*co*-HFP solution and the bore liquid were pressed through the spinneret, in such a manner, that the PVDF-*co*-HFP solution flowed through a ring nozzle, while the coagulating liquid was fed through the inner tube as shown in Figure 1. The composition and the spinning conditions of the fabricated hollow fiber PVDF-*co*-HFP membranes are summarized in Table I. The bore fluid was simultaneously supplied by using a precision gear pump (Information Technology Engineering Co., Guro-Gu, South Korea) to the inner tube of the spinneret at a flow rate of 0.38 mL/min. Both the bore liquid and the external coagulant were pure water. All nascent fibers were not extended by drawing which means that the windup velocity of the hollow fiber was the same as the free falling velocity in the coagulation bath. For the PVDF-*co*-HFP/ PEG/DMAC system, further increase in PEG concentration more than 20 wt% needs to use different spinning conditions of the PVDF-*co*-HFP hollow fibers such as bore fluid flow rate and
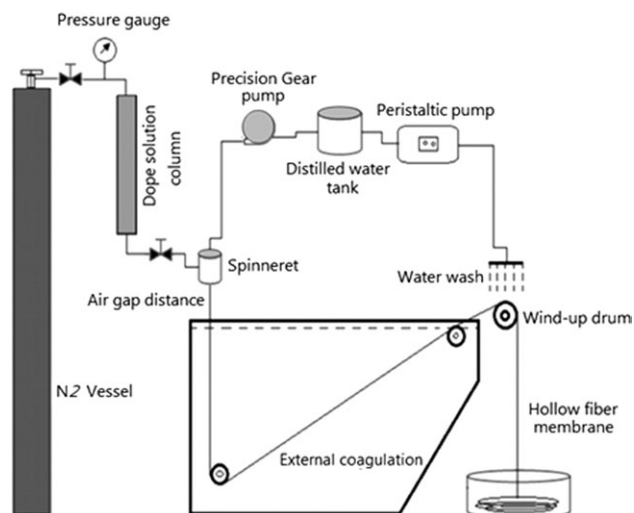

Figure 1. Schematic diagram of the hollow fiber membrane spinning system.

nitrogen gas extrusion pressure due to the significant increase of polymer solution viscosity. The residual solvent was removed by immersing the hollow fibers in a sufficient quantity of pure water for 24 h at 35°C. After that the hollow fibers were transferred to another water bath at 40°C in order to insure that the PEG was removed from the hollow fibers. It is believed that the residual solvent and PEG should then be removed completely from the fibers.

SEM Characterization and Dimension Measurement of Hollow Fiber Membrane Surface
The inner and outer diameters of the prepared poly (ether sulfone) (PES) hollow fibers were measured by using an optical microscope. At least five samples for each hollow fiber were tested.

To visualize hollow fiber membrane surface characteristics, SEM measurements were made using a Philips XL30 FEG instrument with an accelerating voltage of 20 keV. Cross sections were prepared by fracturing the hollow fiber membranes in liquid nitrogen. Hollow fiber membranes samples were coated with a conductive coating (60% gold and 40% palladium) under vacuum in a sputtering system. The conductive coating process was used to eliminate surface charging. The SEM images of the cross

Table I. Spinning Parameter and Operating Conditions of the PVDF-*co*-HFP Hollow Fibers

Spinning parameter	Operating condition
PVDF-*co*-HFP/PEG/DMAC	(20 : 0 : 80), (20 : 5 : 75), (20 : 7 : 73), (20 : 10 : 70), (20 : 12 : 68), (20 : 15 : 65), (20 : 18 : 62), and (20 : 20 : 60)
Internal coagulation temperature	45°C
External coagulation temperature	45°C
Air-gap distance	0.5 cm
Extrusion pressure	3 bar
Bore fluid flow rate	0.38 mL/min

Table II. Inner and Outer Diameter and Porosity of the PVDF-*co*-HFP Hollow Fiber Membranes

Membrane code	PVDF-*co*-HFP/PEG/DMAC Solution (wt %)	ID (mm)	OD (mm)	Thickness (mm)	Porosity (%)
M0	20 : 0 : 80	0.8416 ± 0.112	0.9833 ± 0.12	0.1425	0.667
M5	20 : 5 : 75	0.7333 ± 0.042	1.033 ± 0.02	0.1025	0.846
M7	20 : 7 : 73	0.7750 ± 0.020	1.041 ± 0.06	0.1375	0.821
M10	20 : 10 : 70	0.780 ± 0.02	1.083 ± 0.051	0.1475	0.879
M12	20 : 12 : 68	0.725 ± 0.073	0.975 ± 0.081	0.1115	0.888
M15	20 : 15 : 65	0.7416 ± 0.055	0.9832 ± 0.062	0.1375	0.870
M18	20 : 18 : 62	0.700 ± 0.04	0.9165 ± 0.125	0.1370	0.846
M20	20 : 20 : 60	0.708 ± 0.051	0.925 ± 0.042	0.1250	0.825

section and internal and external surfaces of the membrane were observed at various magnifications.

AFM Characterization of Hollow Fiber Membrane Surface
Each hollow fiber was subjected to extensive surface analysis using an AFM of (Angstrom Advanced Inc., Braintree, Boston, USA) model AA3000, in contact mode with a suitable silicon tip. Measurements included an assessment of the topography (the rise and fall of the sample surface), the lateral force (friction forces between tip and sample, which causes the torsion of the cantilever and can be reflected by the photodetector's left–right signal), and deflection (cantilever flexes because of the rise and fall of sample topography and the amount of this deflection can be reflected by the photodetector's up–down signal). By using IMAGER 4.31 software, a statistical pore size distribution was established for the outer surfaces of each hollow fiber.

Porosity Measurement
The membrane porosity, ε_m (%), can be defined as the volume of the pores divided by the total volume of the membrane. The void fraction of the fibers was determined according to the commonly used method based on density measurements.[9] The void fraction was calculated according to the following equation:

$$\varepsilon_m(\%) = \left(1 - \frac{\rho_{\text{membrane}}}{\rho_{\text{PVDF-co-HFP}}}\right) \times 100, \tag{1}$$

where ρ_{membrane} and $\rho_{\text{PVDF-HFP}}$ are the densities of the membrane and the PVDF-*co*-HFP pellets, respectively. The membrane density was calculated from the mass and volume ratio:

$$\rho_{\text{membrane}} = 4m/\pi \cdot (\text{OD}^2 - \text{ID}^2) \cdot l, \tag{2}$$

where l is the membrane length, m is the mass of the membrane, and ID and OD are the inner and the outer diameters,

respectively. The density of PVDF-*co*-HFP is taken as 1.78 g/cm^3 as reported in Sigma–Aldrich technical sheets.

Solubility Parameter Difference ($\Delta\delta$)
Solubility parameters of the solvent, PEG-600Mw, and PVDF-*co*-HFP were obtained from the literature.[10–12] The solubility parameter difference between PVDF-*co*-HFP and a solvent and the solubility parameter difference between PEG-600Mw and a solvent were calculated from the following equations:

$$\Delta\delta_{\text{S-Polymer}} = \left[\left(\delta_{d,S} - \delta_{d,\text{Polymer}}\right)^2 + \left(\delta_{p,S} - \delta_{p,\text{Polymer}}\right)^2 + \left(\delta_{h,S} - \delta_{h,\text{Polymer}}\right)^2\right]^{0.5} \tag{3}$$

$$\Delta\delta_{\text{PEG-Water}} = \left[\left(\delta_{d,\text{PEG}} - \delta_{d,\text{Water}}\right)^2 + \left(\delta_{p,\text{PEG}} - \delta_{p,\text{Water}}\right)^2 + \left(\delta_{h,\text{PEG}} - \delta_{h,\text{Water}}\right)^2\right] \tag{4}$$

$$\Delta\delta_{\text{S-Water}} = \left[\left(\delta_{d,S} - \delta_{d,\text{Water}}\right)^2 + \left(\delta_{p,S} - \delta_{p,\text{Water}}\right)^2 + \left(\delta_{h,S} - \delta_{h,\text{Water}}\right)^2\right], \tag{5}$$

where the subscripts d, p, and h represent the dispersion, polar, and hydrogen-bonding components, respectively, of the pure component; the subscript S represents the solvent DMAC.

RESULTS AND DISCUSSION

The inner and outer diameters, the thickness, and the porosity of the PVDF-*co*-HFP/PEG hollow fibers prepared under different PEG concentrations in the polymer solution are summarized in Table II. It can be noticed that there are no significant effects of the PEG concentration in the polymer solution on the outer diameters of the prepared hollow fiber membranes. This phenomenon is attributed to the effect of the air-gap distance used during all the spinning experiments. Through the

Table III. Solubility Parameters and Their Differences [(MPa)$^{0.5}$]

Component	δ_d [(MPa)$^{0.5}$]	δ_p [(MPa)$^{0.5}$]	δ_h [(MPa)$^{0.5}$]	$\Delta\delta_{\text{S-Polymer}}$ [(MPa)$^{0.5}$]	$\Delta\delta_{\text{PEG-Water}}$ [(MPa)$^{0.5}$]	$\Delta\delta_{\text{S-Water}}$ [(MPa)$^{0.5}$]
DMAC	16.8	11.5	10.2			32.54
Water	15.5	16.0	42.4			
PVDF-*co*-HFP	17.2	12.5	8.20	2.271		
PEG-600Mw	15.3	9.60	8.50	2.958	34.5	

WILEYONLINELIBRARY.COM/APP

WILEY ONLINE LIBRARY

3 cm air-gap distance, there is a gravitational force effect on the nascent hollow fiber, which induced elongation and stretching of the nascent PVDF-*co*-HFP hollow fibers. In this way, the effect of the 3 cm air-gap distance overcomes the effect of the PEG concentration on the hollow fiber mem-branes dimensions. Alsalhy et al.[9] reported that the outer diameter of the PVC hollow fibers was the same, because the effect of a 4 cm air-gap distance overcomes the effect of PVC concentration in the polymer solution. Regarding the inner diameter, it can be seen from Table II that all the inner
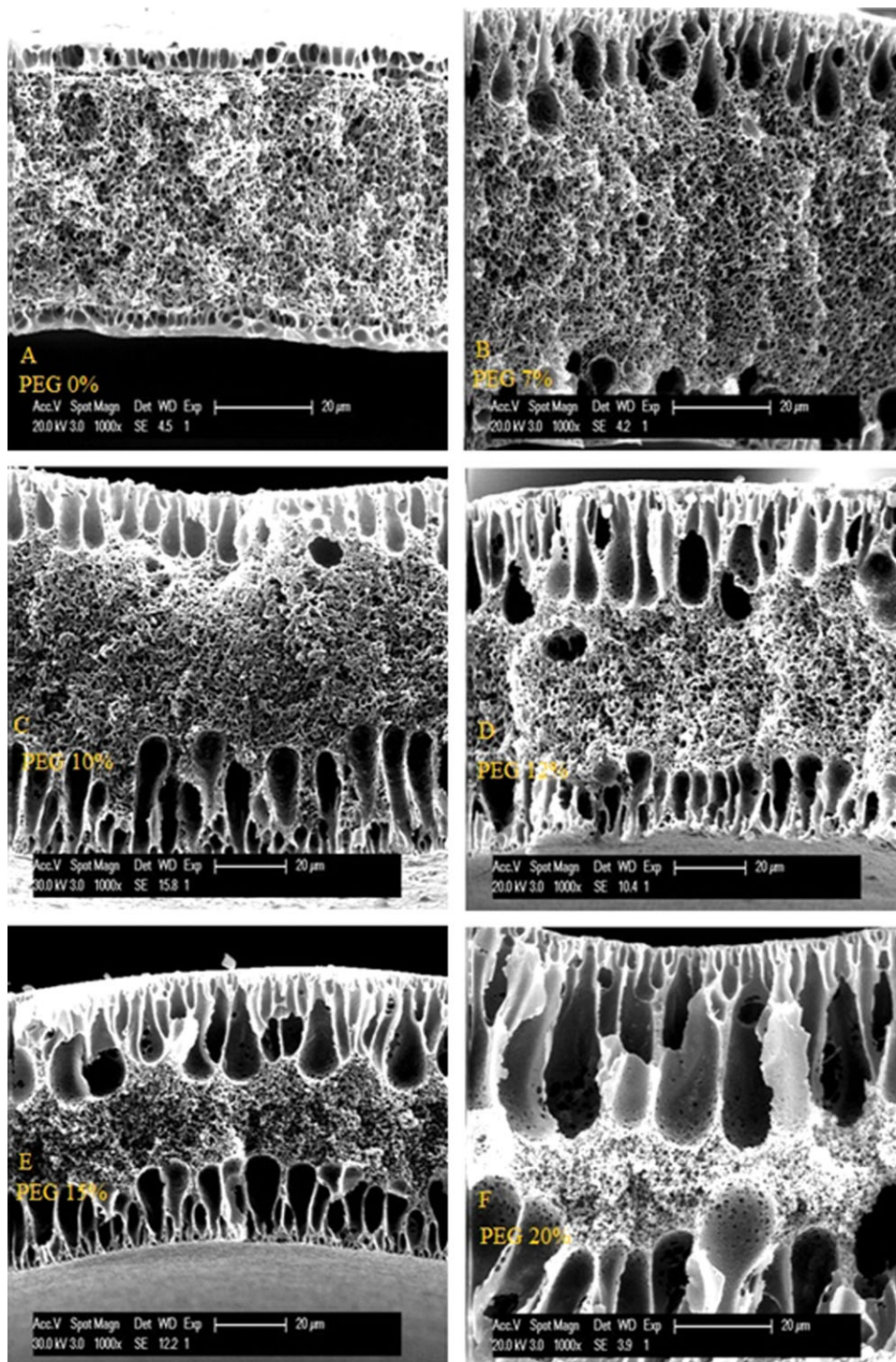

Figure 2. SEM images of the PVDF-*co*-HFP hollow fiber cross section using different PEG concentrations: (A) 0 wt % PEG, (B) 7 wt % PEG, (C) 10 wt % PEG, (D) 12 wt % PEG, (E) 15 wt % PEG, and (F) 20 wt % PEG. [Color figure can be viewed in the online issue, which is available at wileyonlinelibrary.com.]

diameters were higher than the inner diameter of the spinneret. Through the spinneret, the polymer solution was subjected to shear stress, and after the polymer solution leaves the spinneret, swelling occurred. Because the inner surface of the polymer solution was directly brought into contact with the internal coagulant (i.e., water), this led to swelling and solidification of the inner surface of the nascent hollow fiber occurred.

This results in an inner diameter of the hollow fibers to be higher than the diameter of the spinneret. No major effect of the PEG concentration on the inner diameters of the hollow fiber membranes was found as shown in Table II.

The porosity of the PVDF-*co*-HFP hollow fiber membranes increases with the increasing of the PEG concentration in the
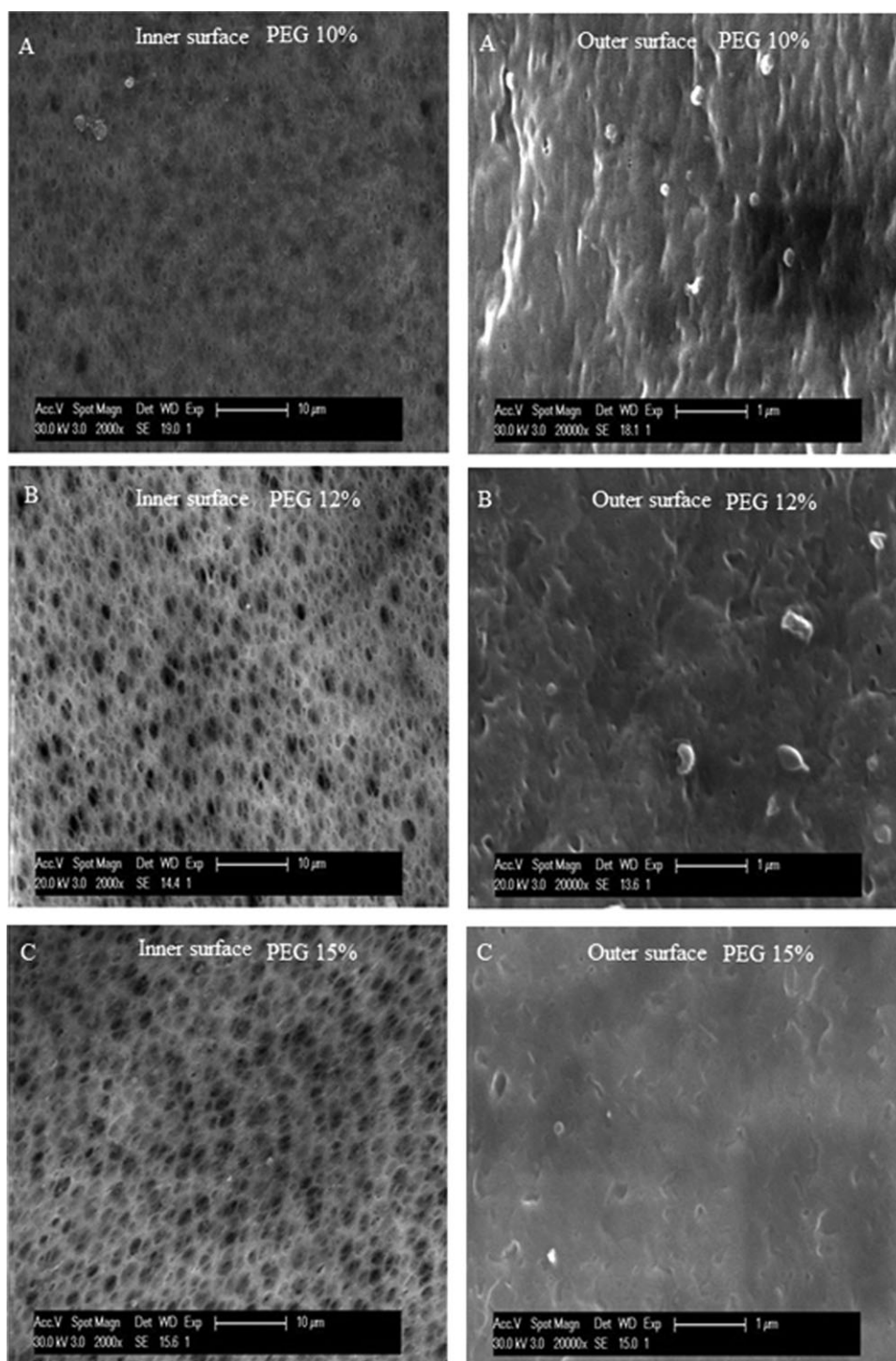

Figure 3. SEM images of the inner and outer surfaces of the PVDF-*co*-HFP hollow fibers using different PEG concentrations: (A) 10 wt % PEG, (B) 12 wt % PEG, and (C) 15 wt % PEG.

polymer solution up to 20 wt % as shown in Table II, whereas the porosity of the hollow fibers prepared from pure PVDF-co-HFP was lower (i.e., $\varepsilon_m = 66.7\%$).

Moreover, from Table II, it can be seen that the porosity of the PVDF-co-HFP reaches a maximum by using 12 wt % PEG in dope solution and then decreases. This behavior is due to the
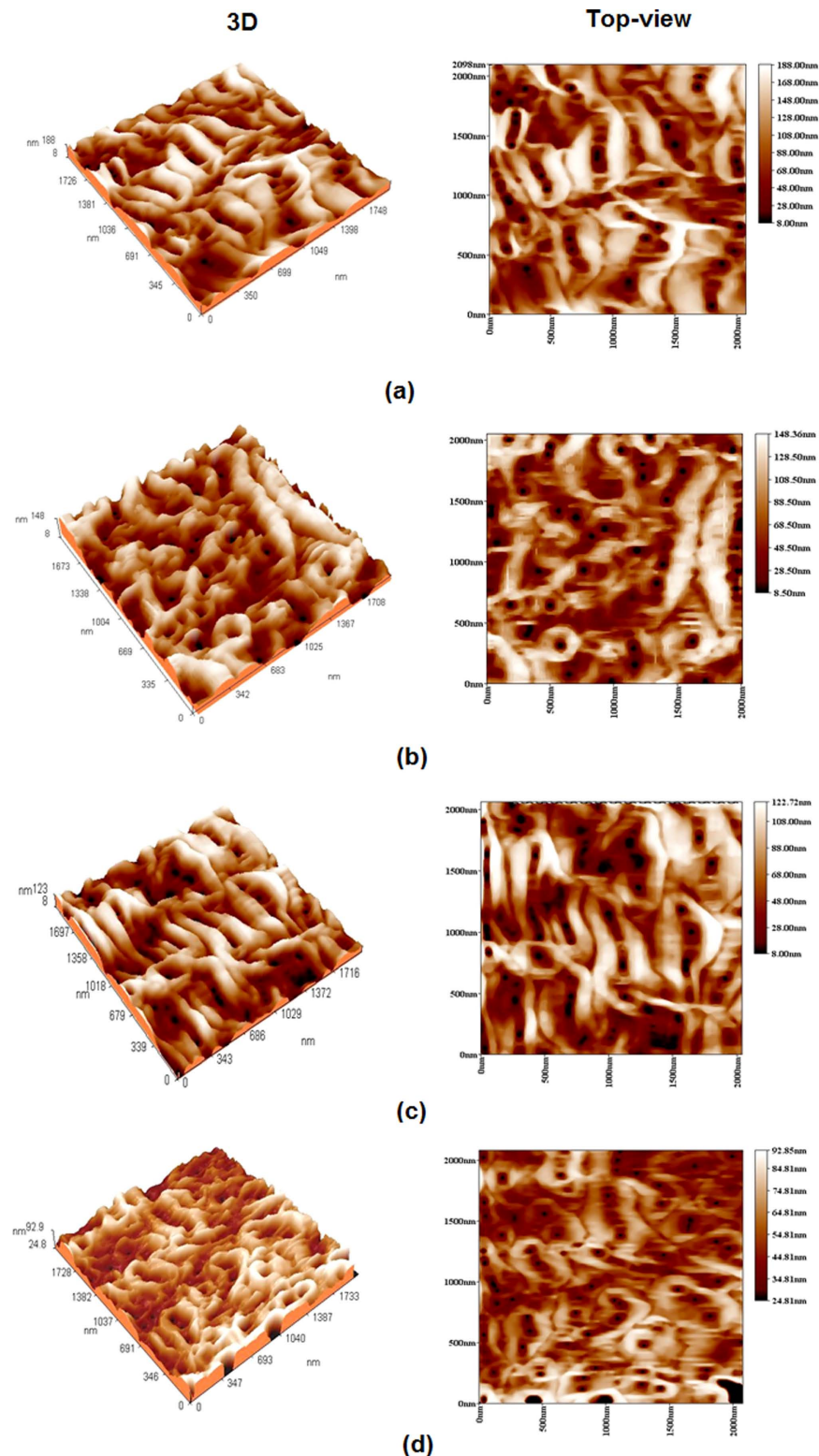
3D   **Top-view**

Figure 4. Topography and three-dimensional AFM images of the outer surfaces of the PVDF-co-HFP hollow fibers prepared at different PEG-600Mw concentrations: (a) 0 wt % PEG, (b) 5 wt % PEG, (c) 7 wt % PEG, (d) 10 wt % PEG, (e) 12 wt % PEG, (f) 15 wt % PEG, (g) 18 wt % PEG, and (h) 20 wt % PEG. [Color figure can be viewed in the online issue, which is available at wileyonlinelibrary.com.]

number of finger-like void, which increases with increase of PEG concentrations up to 12 wt % and then decreases with farther increase of PEG concentration in PVDF-*co*-HFP dope solution. Zheng et al.[13] reported that the porosity of hollow fiber membrane was found to correlate well with the kinetics parameter of membrane formation repeatedly. It can be concluded that the porosity of the membrane can be strongly affected by the addition of the PEG concentration in the polymer solution.

In this case, the morphology of the produced PVDF-*co*-HFP hollow fibers membrane is discussed according to the effect of the different concentrations of PEG (0, 5, 7, 10, 12, 15, 18, and
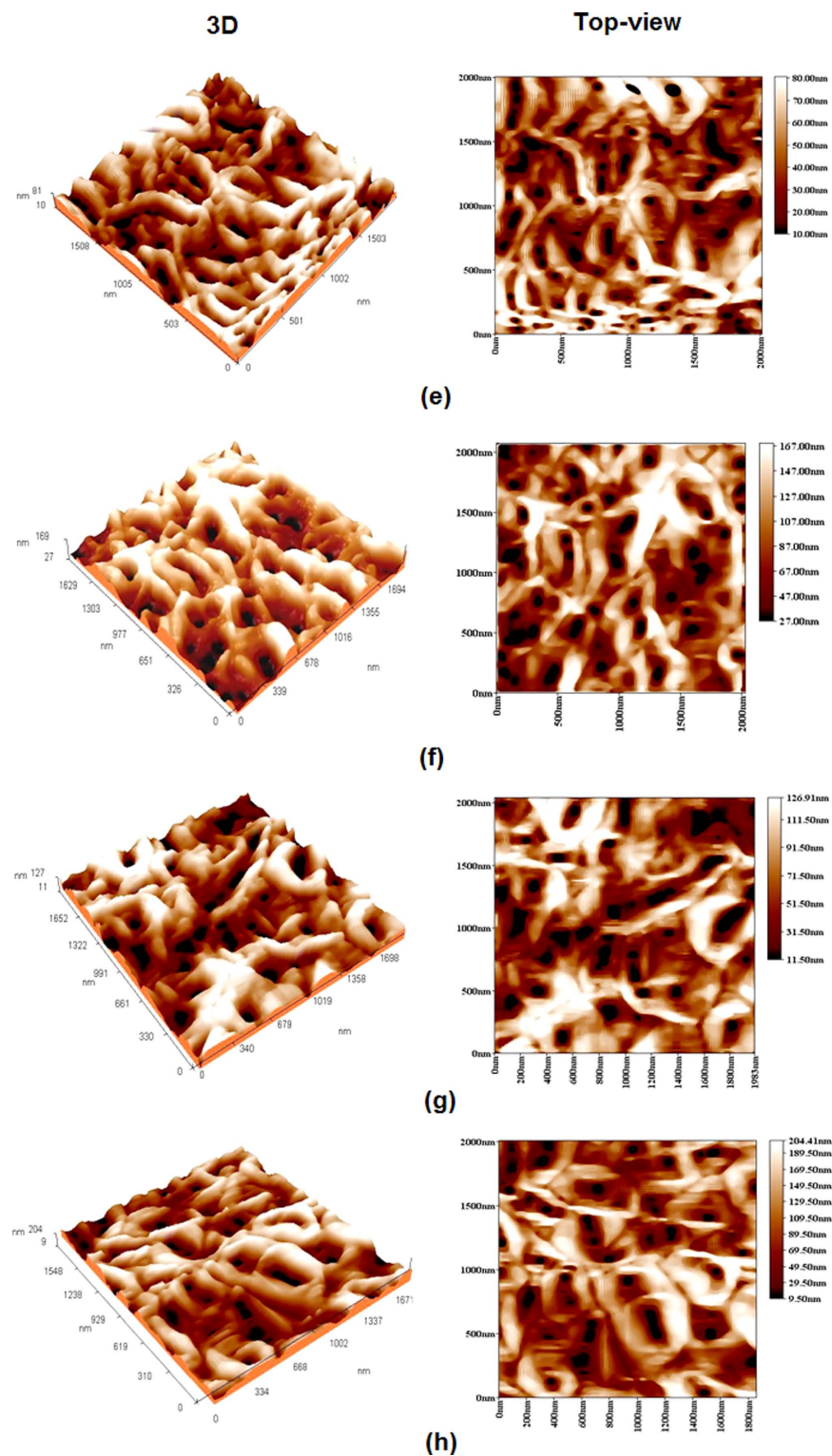

Figure 4. Continued.

Table IV. Mean Pore Size and Mean Roughness of the PVDF-*co*-HFP Hollow Fiber Membranes

Membrane code	PVDF-*co*-HFP/ PEG/DMAC Solution (wt %)	Mean pore size (nm)	Outer surface roughness (5 × 5 μm^2)		
			Mean roughness (R_a)	The root mean square of Z values (R_{ms})	Maximum roughness (R_{max})
M0	20 : 0 : 80	99.12	96.5724	127.722	941.833
M5	20 : 5 : 75	138.59	37.7137	47.8606	332.145
M7	20 : 7 : 73	143.82	34.3381	44.3611	325.429
M10	20 : 10 : 70	168.19	33.3239	43.5893	321.371
M12	20 : 12 : 68	222.75	31.9213	42.6604	384.186
M15	20 : 15 : 65	173.72	27.4091	38.5306	416.469
M18	20 : 18 : 62	352.33	31.4801	42.7857	394.668
M20	20 : 20 : 60	368.91	53.9769	67.636	499.473

20 wt %) in the PVDF–HFP solution. Figure 2 shows the effect of PEG concentrations on the cross-sectional area of PVDF-*co*-HFP hollow fiber membranes. A sponge-like structure can be observed in the cross section of the PVDF-*co*-HFP hollow fibers prepared without PEG as additive, with small cavities that appear near the inner and outer edge of the hollow fibers. Addition of PEG in the polymer solution induces the formation of finger-like voids. Moreover, from Figure 2, it can be noticed that the finger-like structured layer near the inner and outer edges of the hollow fibers increases with increase of PEG concentration in the polymer solution from 5 to 20 wt %. The dimensions of the finger-like macrovoids that appear near the inner and outer edge of the hollow fibers increase toward the middle of the cross section with increase of the PEG concentration in the polymer solution.

The literature confirms that the addition of PEG, which is used as a pore former, may provoke the formation of finger-like structures and macrovoids at the inner and outer edge of the hollow fibers.[3,8] This phenomenon is attributed to two causes: first, PEG increases the thermodynamic instability of the polymer solution, accelerating the diffusion flow of the solvent and nonsolvent throughout the phase inversion process. The solubility parameter difference between PEG and DMAC is higher than that between PVDF-*co*-HFP and DMAC, as shown in Table III. This means that the overlap of PEG chains with DMAC is weaker than PVDF–HFP with the DMAC, which leads to a fast diffusive flow of the solvent and water. Second, the bore liquid was applied at 45°C, and the external coagulant temperature induces the formation of a large finger-like macrovoid structure. Wongchitphimon et al.[8] found that the addition of PEG into the PVDF-*co*-HFP/1-methyl-2-pyrrolidone (NMP) solution results in a thermodynamically instable system in reaction with water, promoting rapid liquid–liquid demixing in the phase inversion process and the formation of larger finger-like structures in the cross section.

SEM images of the inner and outer surfaces of the PVDF-*co*-HFP hollow fiber membranes prepared from different PEG concentrations (i.e., 10, 12, 15 wt %) in polymer solution as additive are shown in Figure 3. It can be seen that there is no evident difference for the outer surface morphologies, and no pores appear at the surfaces even at a magnification of 20,000.

Looking at the inner surfaces of Figure 3, it can be noticed that the pore size and pore density increased with an increase of PEG concentration in polymer solution. Moreover, the microporous structure at the inner surface becomes more uniform and clear, with a narrow pore size distribution when the PEG concentration increases, as shown in Figure 3(A–C), and this is valid for all PEG concentrations. The phenomenon can be explained by the addition of PEG which increases the pore volume of the membrane.

Three dimensions and top-view AFM images of the outer surface over an area of 2 × 2 μm^2 for hollow fiber membranes prepared from different PEG-600Mw (pore-forming) concentrations in polymer solution are shown in Figure 4. It can be seen that the nodular structure is formed in the outer skin of PVDF-*co*-HFP hollow fiber membranes with interconnected cavity channels between the agglomerated nodules on the outer membrane surface. However, a previously undescribed shape of the nodules with different sizes was observed in the outer surface of the PVDF-*co*-HFP hollow fiber membranes prepared by using different PEG-600Mw concentrations in polymer solution. This nodule shape may be denoted as a "twisted rope nodules." The twisted rope nodules size and their wall thickness increase with the PEG concentration in the polymer solution from 0 to 20 wt %, as shown in Figure 4(a–c). A further increase in PEG results in an increase of the twisted rope nodule size with decrease of twisted rope wall thickness, as clearly shown in Figure 4(d–h). Two different phase separation mechanisms take place during the formation of the hollow fiber membrane skin when a homogeneous solution becomes thermodynamically unstable: nucleation and growth (i.e., delay liquid–liquid demixing process) or spinodal decomposition (i.e., fast liquid–liquid demixing process). It is believed that these two mechanisms take place during the formation of the PVDF-*co*-HFP hollow fiber skin. Delay liquid–liquid demixing process takes place during the formation of the membranes prepared from PVDF-*co*-HFP/DMAC/PEG solution resulting in inner surfaces that are fully porous, as shown in Figure 3(A–C). In contrast, fast liquid–liquid demixing takes place during the formation of the membranes prepared from PVDF-*co*-HFP/DMAC/PEG solutions resulting in an outer surface with nodules regardless of PEG concentration.[14] The differences in speed of the liquid–liquid demixing process at the outer surface of the PVDF-*co*-HFP
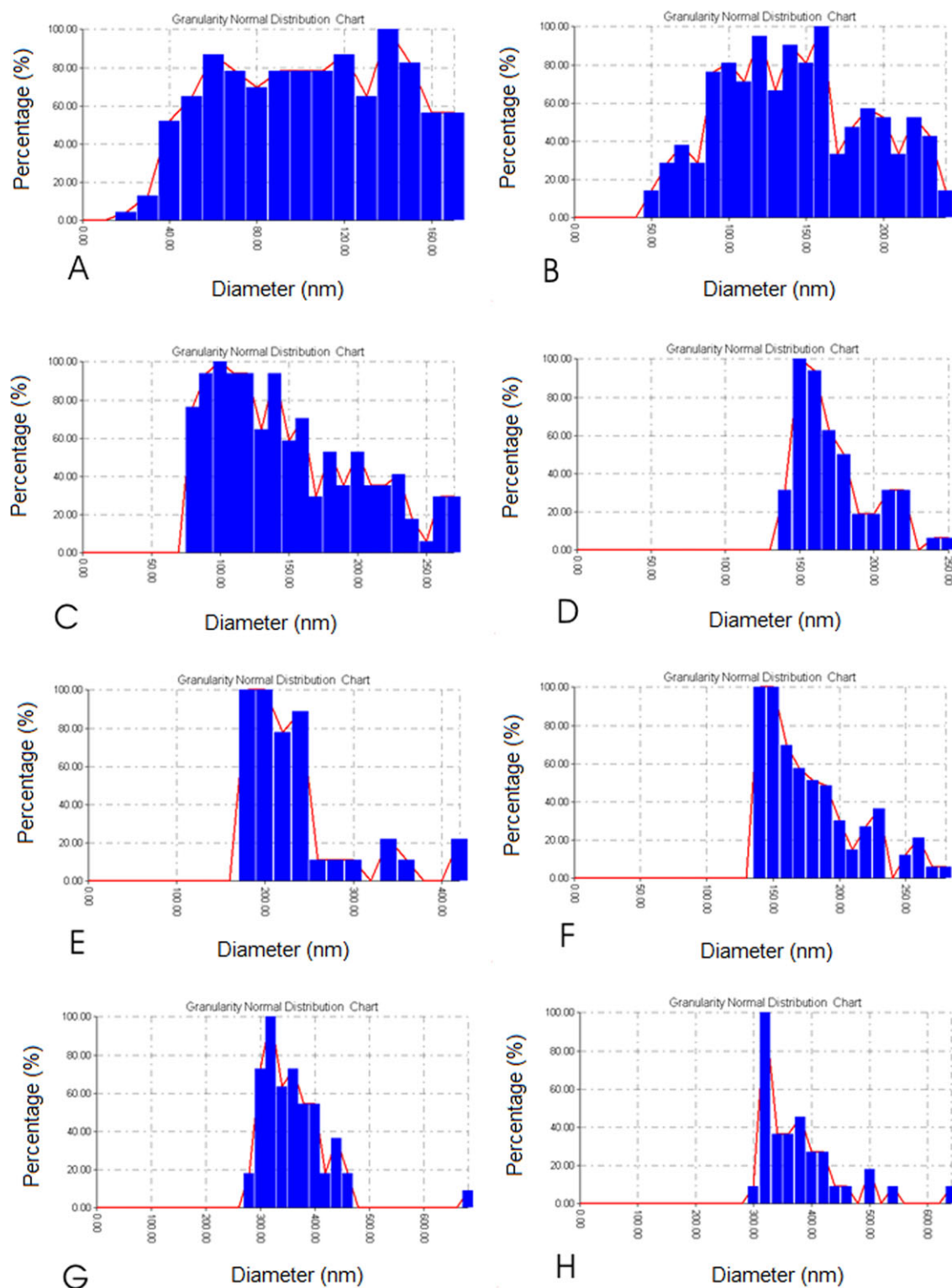
Figure 5. Pores normal distribution chart of the outer surface of the PVDF-*co*-HFP hollow fibers: (A) 0 wt % PEG, (B) 5 wt % PEG, (C) 7 wt % PEG, (D) 10 wt % PEG, (E) 12 wt % PEG, (F) 15 wt % PEG, (G) 18 wt % PEG, and (H) 20 wt % PEG. [Color figure can be viewed in the online issue, which is available at wileyonlinelibrary.com.]

hollow fibers are affected by the PEG concentration, which in turn depends on the pore size and pore size distribution. The outer surface of the hollow fiber prepared from pure PVDF-*co*-

HFP had a small pore size as shown in Figure 4(a) (top-view). The addition of PEG as a pore former in the polymer solution results in an increase of the pore size of the outer surface as

shown in Figure 4(a–h) (top-view). The exchange rate of DMAC/PEG and water plays a very important role to the formation of the outer skin of the PVDF-co-HFP hollow fiber membranes. A higher exchange rate of DMAC/PEG and water results in a porous skin layer due to the effect of PEG as a pore former. The solubility parameter difference between the two polymers and DMAC, as well as between PEG and DMAC and water shown in Table III, supports this behavior.

The mean pore size, the mean roughness (R_a) (the mean value of the surface relative to the center plane), the root mean square of Z values (R_{ms}), maximum roughness (R_{max}) (vertical distance between the highest peaks and the lowest valleys), and pore size distribution of the outer surfaces of the hollow fiber membranes as evaluated over an area of 5×5 μm^2 are shown in Table IV and Figure 5. It can be seen that the mean roughness of the hollow fiber prepared from pure PVDF-co-HFP was the largest, compared with all hollow fiber membranes prepared in this study. This is due to the slower coagulation rate of the surface during the phase inversion process as reported by Khayet et al.[6] In addition, it can be noticed that the mean surface roughness of the hollow fiber membranes decreased with an increase of PEG concentration in the polymer solution. This phenomenon is attributed to the exchange rate of PEG in polymer solution (outflow from dope solution) with nonsolvent water (internal and external coagulant). The exchange rate increases with an increase of the amount of PEG in the polymer solution, which in turn induces pore formation with a uniform and narrow pore size distribution. Moreover, the decrease of the depressions and peaks as shown in Figure 4 (top-view) supports this phenomenon.

Regarding the mean pore size and pore size distribution of the PVDF-co-HFP hollow fiber membranes, it can be seen from Table IV and Figure 5 that the mean pore size increases due to the increase of the PEG concentration in the polymer solution as discussed above based on the SEM images. From Figure 5(A), it can be noticed that a wide pore size distribution is obtained for the hollow fibers prepared without PEG as a pore former. With increase of PEG in the polymer solution, the pore size gradually increases with a narrow pore size distribution as shown clearly in Figure 5(B–H).

In general, the usual characteristic values of hydrophobic membranes used for MD are a mean pore size of 0.1–1.0 μm, a porosity of 40–90%, and a thickness of 20–200 μm.[15] Thus, as can be seen from Tables II and IV, the hollow fiber membranes prepared in this work using PVDF-co-HFP with 5–20 wt % PEG as a pore former are suitable for the application in MD.

CONCLUSIONS

PVDF-co-HFP hollow fiber membranes for MD application were successfully prepared without and with different PEG-600Mw concentrations as a pore-forming additive.

There is no major effect of the PEG concentration on the dimensions of the hollow fibers, whereas the porosity of the

hollow fibers increases the PEG concentration. The cross-sectional structure changed from a sponge-like structure observed on the cross section of the hollow fibers prepared from pure PVDF-co-HFP with small cavities appearing near the inner and outer edges of the hollow fibers to a finger-like structure with a small sponge-like layer in the middle of the cross section. The dimensions of finger-like layers appearing near the inner and outer edges of the hollow fiber increased toward the middle of the cross section with increase of the PEG concentration in polymer solution. This change was attributed to the acceleration of the diffusive flow of the solvent and nonsolvent throughout the phase inversion process due to the presence of PEG as additive at 45°C. A new shape of the nodules, denoted as "twisted rope nodules," with different sizes in the outer surfaces was observed. The mean surface roughness of the hollow fiber membranes decreased with an increase of PEG concentration in the polymer solution. The pore size of the hollow fibers gradually increased with narrow pore size distribution with increase of PEG concentration as a pore former in the polymer solution.

REFERENCES

1. Feng, C.; Shi, B.; Li, G.; Wu, Y. *Sep. Purif. Technol.* **2004**, *39*, 221.

2. Feng, C.; Shi, B.; Li, G.; Wu, Y. *J. Membr. Sci.* **2004**, *237*, 15.

3. Feng, C.; Wang, R.; Shi, B.; Li G.; Wu, Y. *J. Membr. Sci.* **2006**, *277*, 55.

4. Garca-Payo, M. C.; Essalhi, M.; Khayet, M. *Desalination* **2009**, *245*, 469.

5. Garca-Payo, M. C.; Essalhi, M.; Khayet, M. *J. Membr. Sci.* **2010**, *347*, 209.

6. Khayet, M.; Cojocaru, C.; Garca-Payo, M. C. *J. Membr. Sci.* **2010**, *351*, 234.

7. Li, N. N.; Fane, A. G.; Ho, W. S. W.; Matsuura, T. Advanced Membrane Technology and Applications; John Wiley & Sons, Inc., Hoboken, New Jersey, **2008**.

8. Wongchitphimon, S.; Wang, R.; Jiraratananon, R.; Shi, L.; Loh, C. H. *J. Membr. Sci.* **2011**, *369*, 329.

9. Alsalhy, Q.; Algebory S.; Alwan, G. M.; Simone, S.; Figoli, A.; Drioli, E. *Sep. Sci. Technol.* **2011**, *46*, 2199.

10. Brandrup, J.; Immergut, E. H. Polymer Handbook [M], 3rd ed.; Wiley, New York, **1989**.

11. Tian, X.; Jiang, X. *J. Hazard. Mater.* **2008**, *153*, 128.

12. Hansen, C. M.; Just, L. *Ind. Eng. Chem. Res.* **2001**, *40*, 21.

13. Zheng, Q.; Wang P.; Yang Y.; Cui D.; *J. Membr. Sci.* **2006**, *286*, 7.

14. Chung, T. S.; Qin, J. J.; Huan, A.; Toh, K. C. *J. Membr. Sci.* **2002**, *196*, 251.

15. Mulder, M. Basic Principles of Membrane Technology; Kluwer Academic Publishers: Dordrecht, The Netherlands, **1996**.